Available online at www.sciencedirect.com
SCIENCE DIRECT®
International Journal of Thermal Sciences 43 (2004) 677–688
International Journal of Thermal Sciences
www.elsevier.com/locate/ijts

Convective heat transfer in a scroll compressor chamber: a 2-D simulation

Kim Tiow Ooi *, Jiang Zhu [1]

School of Mechanical and Production Engineering, Nanyang Technological University, 50, Nanyang Avenue, Singapore 639798, Singapore

Received 9 July 2003; accepted 12 November 2003

Available online 13 February 2004

Abstract

Literature shows that there is no comprehensive study available on convective heat transfer in a scroll compressor. In this paper, a two-dimensional model has been developed to study the fluid flow and heat transfer in the working chamber of the scroll compressor. The unsteady continuity, momentum and energy equations for the gas flow in the scroll chamber were formulated. The curvilinear, moving and deforming scroll chamber was modeled employing the body-fitted coordinate grid by applying a "two-boundary" algebraic method. The computation accounted for the effect of simultaneous change in the instantaneous volume (volumetric size) and the moving boundary (geometrical shape) of the scroll chamber. With the aid of an available CFD code, the convective heat transfer has been calculated using a standard k–ε turbulence model with a log-law wall function. Results show that available empirical correlations with lumped parameter approach are inadequate in predicting heat transfer within the scroll compressor chamber. This is due to higher heat transfer as a result of the re-circulating flow, in particular, during the later period of the compression process. Results showed that gas properties in the chamber, except the pressure, are highly spatially distributed.

Keywords: Scroll compressor; Convective heat transfer; Fluid flow; Turbulent; 2-D simulation; Deformable-moving boundary

1. Introduction

Ever since its successful implementation in a commercial air conditioning system in 1987, the scroll compressor has become one of the most promising positive displacement compressors for the refrigeration, air-conditioning and heat pump applications in the market today. Most current thermodynamics analysis and simulation employed the lumped parameter approach to model the working process of the scroll compressor [1–5]. More comprehensive understanding on the various aspects of its working process, for example, fluid flow and heat transfer phenomena become necessary in order to increase the accuracy of simulation and performance prediction. Stosic and Smith [6] carried out first numerical simulation on unsteady, multi-dimensional, turbulent and compressible fluid flow in a scroll compressor chamber by separating out the motions of the fluid and the instantaneous volume in which it is contained. However, until today, very little information is available in the open literature that related to the convective heat transfer within the scroll compressor working chamber mainly because of its level of complexity. For the sake of simplicity, most thermodynamic analysis [1–5] neglected the effect of heat transfer or used empirical heat transfer correlations to calculate the heat transfer in the scroll chamber in the lumped parameter models. Direct experimental determination of heat transfer coefficient also presents a great challenge because of small space for measurement, higher position-dependent phenomenon, and high rotating speed of the scroll wrap. For traditional reciprocating machines like compressor and engines, a variety of empirical correlations [7–9] have been developed to evaluate the instantaneous heat transfer. However, there exist significant discrepancies among those empirical models in predicting the heat transfer for different compressors. Furthermore, these empirical correlations take only spatially-average quantities into account and are not suitable for thermal stress deformation analysis of scroll compo-

* Corresponding author.
E-mail addresses: mktooi@ntu.edu.sg (K.T. Ooi), jiangzhu@rice.edu (J. Zhu).
[1] Current address: Department of Mechanical Engineering and Materials Science, MS 321, Rice University, 6100 Main Street, Houston, TX 77005, USA.

1290-0729/$ – see front matter
doi:10.1016/j.ijthermalsci.2003.11.005

Nomenclature

A	area	m^2	
C_f	skin friction coefficient		
C_p	specific heat (constant pressure)	$J{\cdot}kg^{-1}{\cdot}K^{-1}$	
d_e	characteristic dimension	m	
h	specific enthalpy	$J{\cdot}kg^{-1}$	
h_c	convective heat transfer coefficient	$W{\cdot}m^{-2}{\cdot}K^{-1}$	
k_ω	turbulent kinetic energy	$m^2{\cdot}s^{-2}$	
m	mass	kg	
Nu	Nusselt number		
P	pressure	$N{\cdot}m^{-2}$	
Pr	Prandtl number		
Q	heat transfer	J	
q	heat flux	$W{\cdot}m^{-2}$	
R	universal gas constant	$J{\cdot}kg^{-1}{\cdot}K^{-1}$	
Re	Reynolds number		
S	source terms		
t	time	s	
T	gas temperature	K	
u	specific internal energy	$J{\cdot}kg^{-1}$	
U^+	friction velocity	$m{\cdot}s^{-1}$	
$\vec{V}$	gas velocity vectors	$m{\cdot}s^{-1}$	
V	y-streamwise velocity components	$m{\cdot}s^{-1}$	
W	z-streamwise flow velocity components	$m{\cdot}s^{-1}$	
v	velocity component	$m{\cdot}s^{-1}$	
w	velocity component	$m{\cdot}s^{-1}$	
y^+	dimensionless distance		
y	distance to wall	m	
y, z	Cartesian coordinates		

Greek symbols

Γ_ϕ	exchange coefficient	
α	flow coefficient	
ε	turbulent dissipation rate	$m^2{\cdot}s^{-3}$
ϕ	conserved variable	
μ	dynamic viscosity	$kg{\cdot}m^{-1}{\cdot}s^{-1}$
μ_{eff}	effective viscosity	$kg{\cdot}m^{-1}{\cdot}s^{-1}$
θ	crank angle	
ρ	gas density	$kg{\cdot}m^{-3}$
σ_t	turbulent Prandtl number	
τ_w	shear stress	$N{\cdot}m^{-2}$
υ	specific volume	$m^3{\cdot}kg^{-1}$
ω	crank angular speed	$rad{\cdot}s^{-1}$

Subscripts

g	grid velocity components arising from mesh motion
i	in
l	leakage
o	out
w	wall
eff	effective quantity

nents. It is worthwhile to study whether these correlations are suited to evaluate the convective heat transfer within the scroll compressor working chamber. In this paper, effort has been made to develop a two-dimensional numerical formulation to simulate the fluid flow and heat transfer with a complex moving and deformable boundary. This research is expected to provide an insight to understand the qualitative and quantitative characteristics of convective heat transfer during the working process of a scroll compressor.

2. Numerical model

2.1. Formulation of governing equations

The control volume of a scroll working chamber consists of a pair of the crescent-shaped scroll wraps. There is mass flow through the suction and discharge ports as well as heat and work interactions inside the compression chamber over a working cycle. As the working processes of the scroll compressor is a transient flow process involving energy and mass change with time, the temporal variation of the gas state is continuously progressing through a series of time interval, i.e., crank angle. The time dependent governing equations based on the conservation of mass, momentum, and energy balance are used to describe the compressible gas flow and heat transfer within the scroll compressor working chamber. The irregular geometry of the scroll compressor working chamber requires the use of the body-fitted curvilinear (BFC) coordinates to represent the physical flow domain.

The ensemble averaged forms of the differential conservation equations include the mass continuity equation, Navier–Stokes equations that govern the conservation of momentum per unit mass (i.e., velocity) in various flow directions, the energy balance equations, turbulent kinetic energy and its dissipation rate equations. For a single phase phenomenon in question, these equations can be presented in a generalized form as given below.

The conservation of mass is given by the continuity equation [10]:

$$\frac{\partial \rho}{\partial t} + \operatorname{div}\left(\rho \vec{V}_\phi\right) = 0 \tag{1}$$

The unsteady Navier–Stokes equation and the energy equation are generalized for compactness into a single source balance equation for any dependent variables ϕ [10]:

$$\frac{\partial}{\partial t}(\rho\phi) + \operatorname{div}\left(\rho \vec{V}_\phi \phi - \Gamma_\phi \operatorname{grad}\phi\right) = S_\phi \tag{2}$$

where the various terms in Eq. (2) are transient, convection, diffusion and source terms respectively, and ϕ is any conserved property such as enthalpy, momentum per unit

Table 1
Definition of ϕ, Γ_ϕ and S_ϕ in conservation and transport equations

Equation	Variable	Exchange coefficient	Source terms
	ϕ	Γ_ϕ	S_ϕ
continuity	1	0	0
y-momentum	V	μ_{eff}	$-\frac{\partial P}{\partial y}$
z-momentum	W	μ_{eff}	$-\frac{\partial P}{\partial z}$
energy	h	$\frac{\mu_{\text{eff}}}{\sigma_h}$	$-\frac{\mathrm{d}P}{\mathrm{d}t}$
turbulent energy	k	$\frac{\mu_{\text{eff}}}{\sigma_{k,t}}$	$P_k - \rho\varepsilon$
dissipation rate	ε	$\frac{\mu_{\text{eff}}}{\sigma_{\varepsilon,t}}$	$\frac{\varepsilon}{k}(C_1 P_k - C_2\rho\varepsilon) + C_3\rho\varepsilon\frac{\partial U_i}{\partial x_i}$

mass and turbulence energy, etc. The S_ϕ is the source terms such as that due to pressure, body force, generation and the dissipation of turbulence energy. In the mathematical formulation, the following simplifications and assumptions were made:

(1) Since the working chamber has a long and narrow geometry, the main flow direction is assumed to be along the scroll spiral direction. The flow can then be simplified as a two-dimensional problem in a horizontal plane (for a vertically installed compressor).
(2) The working gas is assumed to be in a single phase and behaves like an ideal gas, the existence of the lubricating oil is neglected.
(3) Constant pressure specific heat and other transport properties are taken as constant.
(4) Gravity force is negligible when comparing with pressure gradient.
(5) There is no leakage across the seal surfaces between the flow domain and surrounding.

Based on the above assumptions, the final formulations of the differential equations are presented in the following section, primarily by replacing ϕ, Γ_ϕ and S_ϕ with the appropriate expressions as shown in Table 1.

In the two-dimensional momentum equations, z-streamwise is selected as the main flow direction along the scroll spiral because of the narrow and long flow domain within the crescent shaped compression chamber. Thus W is the streamwise velocity component in the dominant direction. The specific enthalpy h is the variable solved in the energy equation. The term $\mathrm{d}P/\mathrm{d}t$ represents the pressure work. In the present analysis, the standard k–ε turbulent model [11] is used to calculate the transport of characteristic length scale and time scale of the turbulent motion.

In the analysis, the state equation of an ideal gas is used as formulated for the auxiliary variable. The gas diffusion term uses a gas conductivity that is a function of viscosity and specific heat. Scroll walls are treated as heat conducting bodies with constant conductivity. The gas specific heat is assumed constant and is taken at the bulk temperature of the compression chamber. In the computation, the temperature field is calculated via algebraic enthalpy-temperature relation from the solution of the total enthalpy.

2.2. Modification of governing equations

In a scroll compressor, the gas compression process is achieved through a continuous geometric volume reduction of the working chamber. The gas is driven and compressed by the "squish motion" of the orbiting scroll wrap. This is a complicated time-varying flow domain problem involving the moving and deforming curvilinear-boundary. The moving boundary cannot be converted to stationary boundaries simply through a transformation of the reference frame. Therefore, the volume motion and deformation must be explicitly included into the problem solution procedures. The conservation equations should be modified so that the effects of the control volume boundary velocities and net convective fluxes are considered. The basic conservation equations for mass, momentum and other scalars are modified as following:

$$\frac{1}{\omega}\frac{\mathrm{d}}{\mathrm{d}t}\rho\omega + \frac{\partial}{\partial y}\rho(V - V_g) + \frac{\partial}{\partial z}\rho(W - W_g) = 0 \tag{3}$$

$$\frac{1}{\omega}\frac{\mathrm{d}}{\mathrm{d}t}\rho\omega\phi + \frac{\partial}{\partial y}\rho(V - V_g)\phi + \frac{\partial}{\partial z}\rho(W - W_g)\phi = \frac{\partial}{\partial y}\Gamma_\phi\frac{\partial\phi}{\partial y} + \frac{\partial}{\partial z}\Gamma_\phi\frac{\partial\phi}{\partial z} + S_\phi \tag{4}$$

where $\mathrm{d}/\mathrm{d}t$ is the total derivative and represents the time variation of change of variable ϕ relative to the moving and deforming mesh:

$$\frac{\partial\omega}{\partial t} = \frac{V^{n+1} - V^n}{\Delta t} = \sum_i (v_i \ell_i) \tag{5}$$

ω is a measure of change of the control volume (i.e., mesh deformation) as it deforms with the moving mesh, V^{n+1} and V^n are the volume of the deforming mesh element in n and $n+1$ time steps, respectively, and ℓ_i is the ith surface boundary segment of the control volume.

2.3. Moving and deforming BFC grid

In the present application, the moving and deforming grid systems were generated by an algebraic grid generation method, which is called "two-boundary technique" based on the transfinite interpolation proposed by Smith [12]. The technique can generate non-uniformly distributed, but stationary grid points in two-or three-dimensional spatial domains of fairly arbitrary shapes. Later, Yang and Shih [13] extended and further developed this two-boundary technique so that in addition to non-uniform distribution, the grid points can also move to adapt the arbitrary mesh deformation in response to motion of the computational boundaries, and the net convective effects can thus be evaluated. Shih [14] applied the method to simulate the two-dimensional flow in a Wankel rotary engine which also has a moving curvilinear

geometry. Since the spatial domain inside a scroll compressor working chamber deforms considerably in shape and size just like that in a rotary engine, this extended method is believed to be suitable for the present problem.

2.4. Boundary conditions

The two-dimensional flow configuration consists of an orbiting wrap wall, a fixed wrap sidewall and two apex seal surfaces. Since the flow domain is closed with no inflow and outflow, only one type of physical boundary conditions are required. The following boundary conditions can be set:

(1) Walls are impermeable to mass diffusion, no slip exists and the gas velocity on the wall surfaces are equal to the wall velocity. The momentum boundary is: $W = 0$; $V = 0$ at stationary wall and $V = \frac{\partial y}{\partial t}$; $W = \frac{\partial z}{\partial t}$ at moving wall.
(2) Kinetic energy and its dissipation rate are based on the assumption of local equilibrium. This is also set through the wall function law.
(3) The gas temperatures on all wall boundaries are equal to those of the walls. Uniform temperature for both fixed and orbiting scroll wall is assumed.
(4) The pressure gradient normal to the wall is set to zero.
(5) There is no leakage across the boundary, hence no inflow and outflow.

2.5. Initial conditions

Gas is assumed to be at a uniform state for initial condition. The gas pressure, temperature and velocity components are set to an average value referring to the simulation results using a lumped parameter approach. The initial values of turbulent energy k and dissipation rate ε are assumed constant over the compression chamber. The k is taken as some percentage of the square of the initial velocity and ε is chosen so that the ratio k/ε, which represents a turbulent time scale, is near 10^{-3} s:

$$k = C_\mu^{-1/2} W^2, \qquad \varepsilon = C_\mu^{3/4} k^{1.5}/\kappa Y \tag{6}$$

2.6. Heat transfer calculation

In order to calculate the heat transfer between the gas and the scroll wrap walls inside the compression chamber, the classical wall function approach in conjunction with standard turbulence model by Tennekes and Lumley [15] was employed. The wall local heat flux q_w can be expressed by the following expressions as presented by Gilaber and Pinchon [16]:

$$q_w = \frac{\mu C_p}{P_r}\frac{\Delta T}{y} \quad y^+ \leqslant 11.6 \tag{7}$$

$$q_w = \frac{\rho C_p k_\omega^{1/2} C_\mu^{1/4} \Delta T}{\frac{\sigma_t}{\kappa}\mathrm{Ln}(Ey^+) + \sigma_t' P(\sigma_t')}, \quad y^+ \geqslant 11.6 \tag{8}$$

where

$$P(\sigma_t) = \frac{\pi/4}{\mathrm{Sin}(\pi/4)}\left(\frac{A}{\kappa}\right)^{1/2}\left(\frac{P_t}{\sigma_t'} - 1\right)\left(\frac{P_t}{\sigma_t'}\right)^{-1/4}$$

and

C_p = specific heat at constant pressure of the fluid

ΔT = temperature difference between the wall and fluid adjacent to the wall

σ_t = turbulence Prandtl number (assumed to be 0.6 in this work)

$\sigma_t' = 0.9$

P_t = laminar Prandtl number (i.e., molecular Prandtl number, 0.7 for air)

A = Van Driest constant (26 for slide duct)

where k is the turbulent kinematics energy in the cell adjacent to the wall, it models the effect of the turbulence and the mean flow field on friction and heat transfer. Other constants are $C_\mu = 0.09$; Von Karman constant $\kappa = 0.42$; logarithmic constant $E = 9.2$; $\nu, \gamma, \tau_w, \rho$ are the molecular viscosity, the shear stress and the density, respectively, y is the distance of the cell adjacent to the wall; y^+ represents the dimensionless distance to the wall which reflects the effect of turbulence pulse

$$y^+ = y\left(C_\mu^{1/4} k_\omega^{1/2}\right)/\gamma \tag{9}$$

The Nusselt number [11] is given by:

$$Nu = \frac{Re\,Pr}{\frac{\sigma_t}{\kappa}\mathrm{Ln}(Ey^+) + \sigma_t' P(\sigma_t')} \tag{10}$$

where $Nu = h_g y/\lambda$, $Pr = C_p\mu/\lambda$ and $Re = C_\mu^{1/4} k_\omega^{1/2} y/\gamma_l$.

The submodel of the heat transfer takes into account both the instantaneous and local characteristic of the turbulent flow. It has been employed in many applications where the predictions showed good agreement with experimental measurement. One of examples is the heat transfer simulation in a motored engine by Gosman [17] and Ikegami [18] where good predictions were obtained as compared to the measured values.

It is also noted that the application of the above expression to the flow inside the chamber of the scroll compressor is an approximation because the flow is unsteady and very complex in nature. Some empirical constants are chosen referring to other research, for an example, the value of σ_t was taken to be 0.6 referring to empirical value used in a study of gas flow in a Wankel engine [14].

3. Numerical results and discussion

The present fluid flow and heat transfer simulation was carried out within a vertical scroll compressor for air conditioning applications. Its geometrical parameters are listed

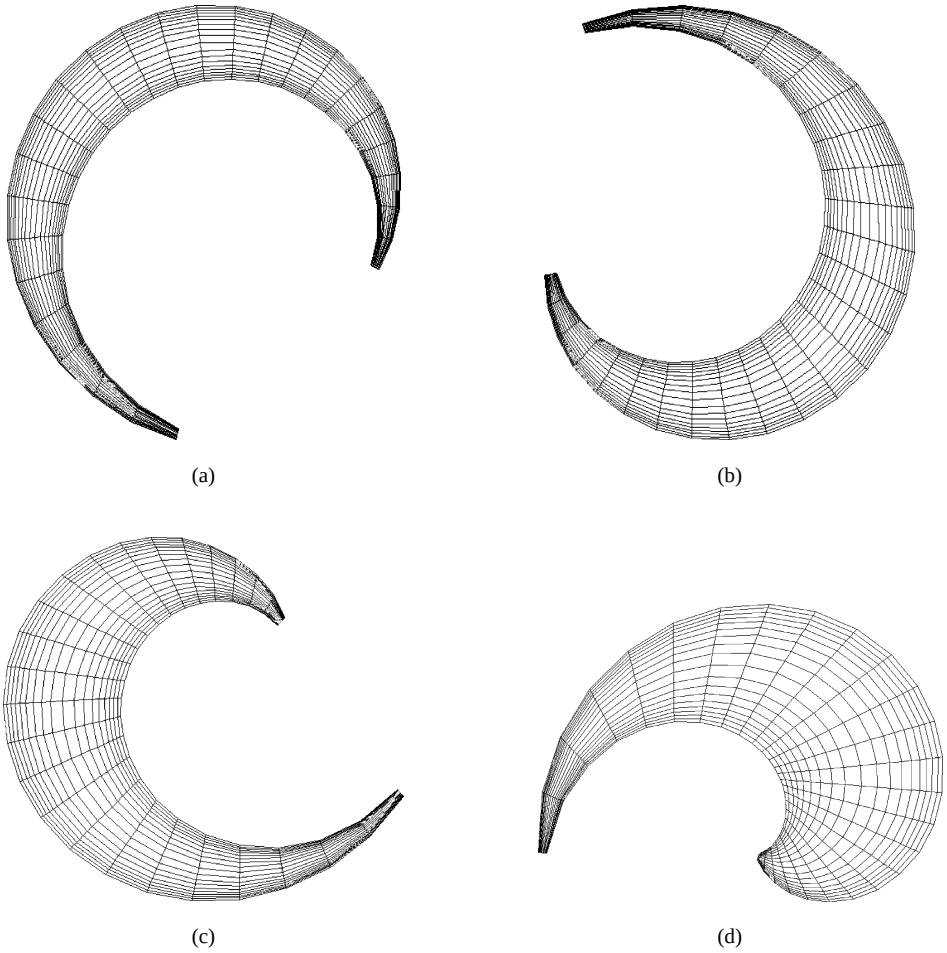

Fig. 1. Grid distribution of the solution domain at some typical angular positions. (a) Grid distribution at crank angle of 60°. (b) Grid distribution at crank angle of 210°. (c) Grid distribution at crank angle of 360°. (d) Grid distribution at crank angle of 510°.

in Table 2. The refrigerant medium is R134a [19]. The typical operating conditions include the intake gas temperature of 300 K at the peripheral port and the suction pressure of 0.35 MPa. In the present study the wall temperature was taken as 330 K. The numerical calculation commenced at the beginning of the compression process and was terminated just before the discharge process begins. It was carried out at each time step over a compression cycle in which the overall crank angular span is about 540°. The convergence is deemed to reach when the maximum sum of the absolute residuals at the end of the iterations is less than 0.1 percent of the value of variables solved so that sufficient accuracy was obtained.

By using the algebraic "two-boundary" technique, grids systems were generated in a time-varying spatial domain inside the scroll compression chamber. Figs. 1(a)–(d) show the grid generation at several typical crank angles. For illustration purpose, these figures are not scaled to actual size of the control volume. The crank angle defines the position of the working chamber. The grid system in the compression working chamber is such that grid spacing changes from the leading apex to the trailing apex and also with time. The orbiting scroll rotates in a counter clockwise direction. The outer boundary line represents the orbiting scroll wrap.

3.1. Pressure

The results of the two-dimensional numerical computations include the local instantaneous gas properties such as the pressure, the temperature, the density and the velocity throughout the working chamber at each computational time step. In general, the results show that all gas properties and convective heat transfer are spatially non-uniformly distributed. This non-uniformity makes the predictions employing the lumped parameters approach using the First Law of Thermodynamics inaccurate. However, the pressure field does not show significant spatial non-uniformity. For example, at the crank angle of 400° the maximum pressure difference among the various locations is less than 200 Pa, which is less than one percent of the average gas absolute

Table 2
Scroll compressor geometry specification

Displacement volume V_{th} [cm^3]	2×67.876
Built-in volume ratio s	2.7
Basic circle radius r [mm]	3.54
Orbiting radius R_o [mm]	11.8
Wrap pitch P_t [mm]	44.52
Wrap thickness t [mm]	5.2
Wrap height h [mm]	23.54

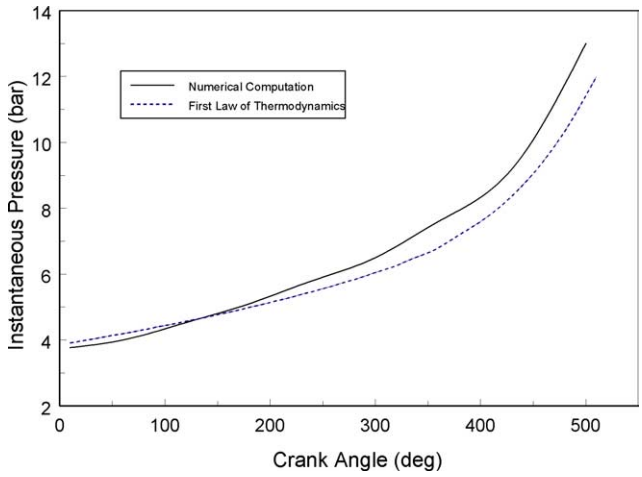

Fig. 2. Comparison of pressure predicted from the numerical simulation and lumper approach.

pressure. This spatial difference of pressure is too trivial to show in contour plots that are not given here. As a conclusion, assumption of uniform chamber pressure is acceptable in all lumped parameter computation. Fig. 2 represents the variation of the bulk gas pressure with crank angle from 2-D simulation and the lumped parameter approach employing the First Law of Thermodynamics. The numerical method predicts a higher value of more than 15%. This discrepancy may be due to the exclusion of the thin-sharp tip of the two apex parts of the chamber to facilitate the computation and results in a smaller chamber volume.

3.2. Velocity

Computations on the flow field were carried out at consecutive time steps over a whole compression cycle. For the purpose of illustrations and discussions, several typical velocity fields in selected crank angle positions are shown. Since there are no significant changes between the consecutive time steps, figures are not displayed to scale in order to facilitate illustration. Figs. 3–7 show the main feature of the flow field inside the compression chamber at a rotating speed of 3000 rev·min.

During the whole compression process as the intake and the exhaust ports are closed, the gas is confined within the compression chamber. It is this orbiting scroll motion that sweeps and drives the gas to flow along the scroll involute toward the center of the compressor in a spirally manner.

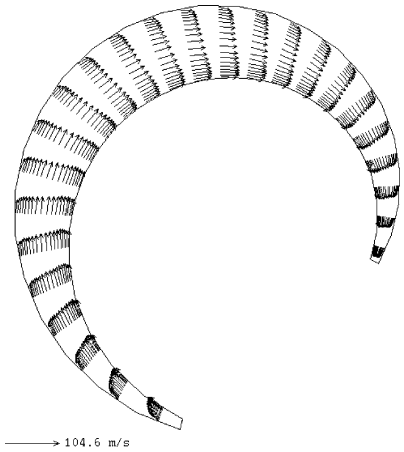

Fig. 3. Flow pattern prediction at crank angle of 60°.

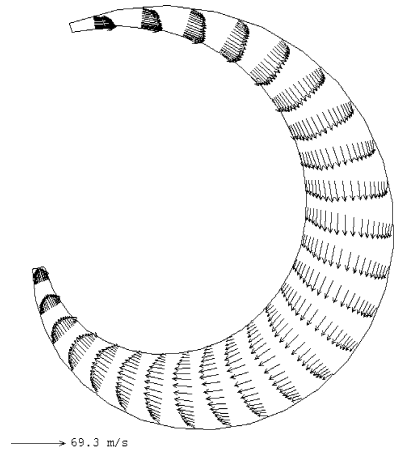

Fig. 4. Flow pattern prediction at crank angle of 210°.

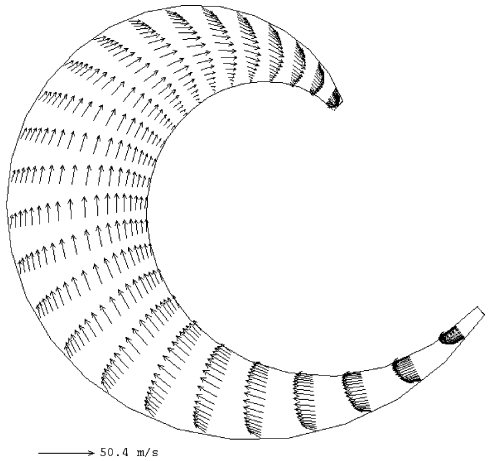

Fig. 5. Flow pattern prediction at crank angle of 360°.

This causes a bulk movement of the gas together with the entire working chamber in one direction. During the early period of the compression cycle, a simple unidirectional flow field is formed from this orbiting scroll induced bulk fluid motion. The mean velocity increases almost monotonically from the stationary scroll surface to the core region and then

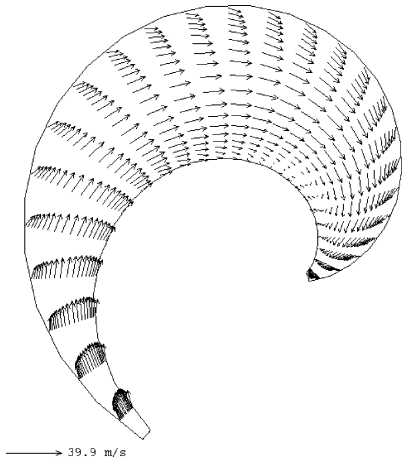

Fig. 6. Flow pattern prediction at crank angle of 450°.

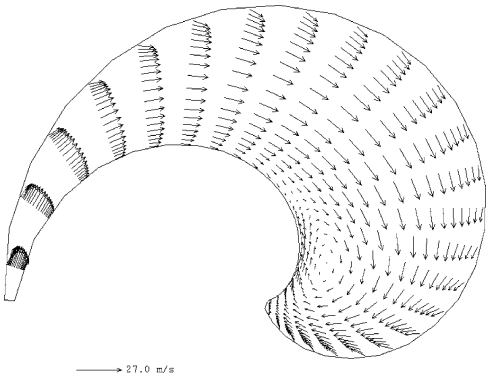

Fig. 7. Flow pattern prediction at crank angle of 510°.

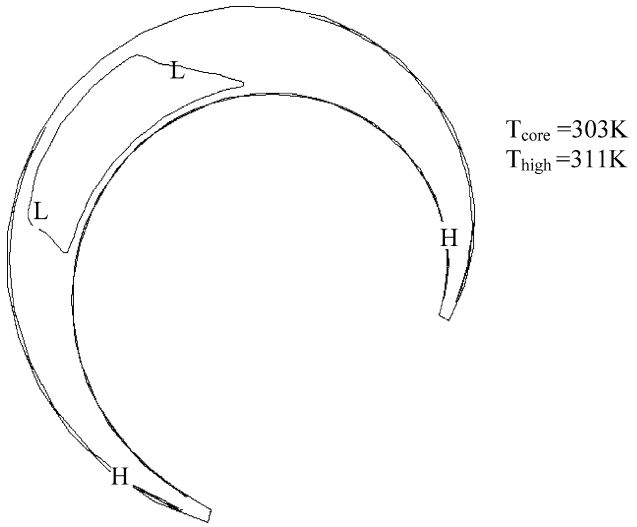

Fig. 8. Temperature distribution at crank angle of 60°.

decreases as it is close to the moving surface. The "squish motion" due to the momentum of the orbiting scroll wrap accelerates the gas near the trailing apex and decelerates the gas near the leading apex. The maximum gas velocity occurs at the center of the chamber. This flow pattern is maintained to be stable and reinforced during the early part of the compression process when the crank angles are less than 420°. This indicates that the nature of the flow field is governed mainly by the scroll chamber geometry and the compression process. Beyond the crank angle of 420°, a recirculating flow began to form near the widest part of the scroll chamber. The overall flow field may be divided into a mainstream flow and a recirculating flow zone. This is because of a highly curved scroll wall that results in a positive pressure gradient as the bulk fluid is driven in the direction of the volume deformation. The momentum induced by the orbiting scroll forces the gas to bend towards the wall. The squish and impingement cause the formulation of the recirculating flow, the strength of which increases with the crank angle. The magnitude of the flow velocity reduces drastically as the working chamber moved towards the inner part of the scroll compressor.

Further discussions of the flow field require consideration of the turbulence characteristics. Velocity fields have shown that there are large gas velocity vector and gradients within the scroll compressor working chamber. In the narrow flow domain, turbulence characteristics would have significant effect on the heat transfer. Computation results indicated that the turbulence intensity is indeed large. In a very small zone near to the wall, the kinetic energy k reaches a maximum value of about 15 $m^2 \cdot s^{-2}$. The dissipation rate is also high near the walls and the two apex regions. Turbulence intensity and diffusivity are larger near the fixed scroll wrap, decrease markedly towards the center of the compression chamber and then rises again near the orbiting scroll. Obviously, the high turbulence kinetic energy and the dissipation rate near the boundary are due to the large gas velocity gradient near the scroll wall surface, which results from the squish action generated by the decreasing of the chamber volume. Turbulent kinetic energy is also high at the regions of high curvature.

3.3. Temperature

In this simulation, the energy conservation equation was solved simultaneously. The temperature fields were obtained by the gas temperature-enthalpy relationship. The gas temperature distribution within the working chamber is shown in Figs. 8–11 at a rotating speed of 3000 $rev \cdot min^{-1}$ and the suction pressure of 0.35 MPa. In plotting this scalar quantity, an increment is selected and remains the same from graph to graph. The letters "L" or "H" indicate the relative magnitude of low and high. Results show that temperature distributions are non-uniform within the compression chamber. This phenomenon is more apparent at the region of two apexes and near the scroll walls. A maximum temperature difference of 8 K was predicted. The gas temperature variation is caused by not only the compression effects but also the convective heat transfer between the gas and the scroll walls. The latter causes the gas temperature near the wall to rise rapidly. During the earlier stage of the compression process, the gas near the

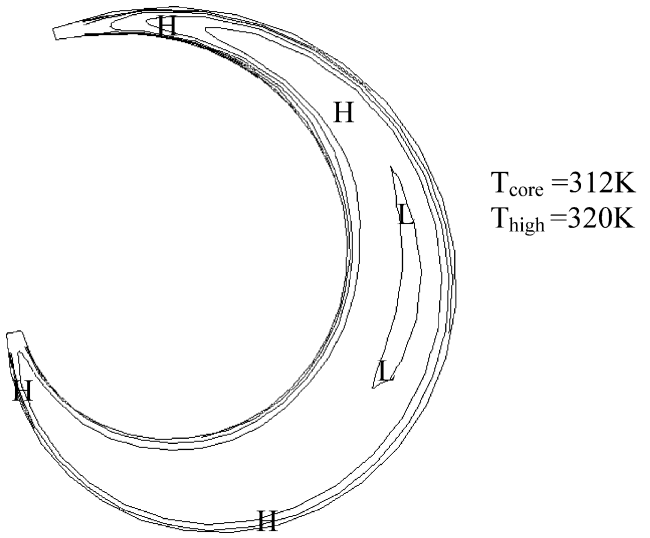

Fig. 9. Temperature distribution at crank angle of 210°.

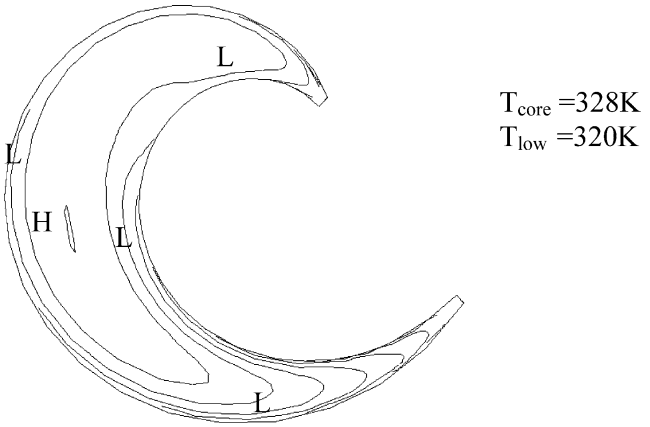

Fig. 10. Temperature distribution at crank angle of 360°.

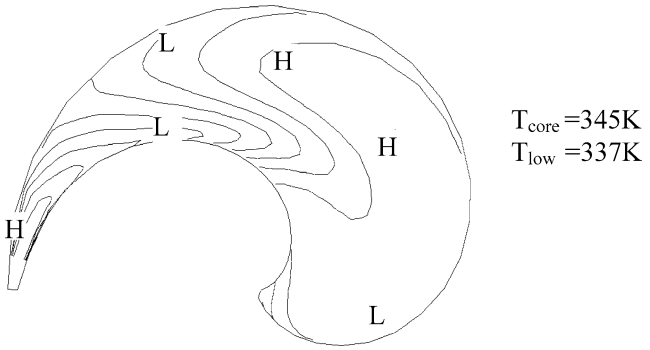

Fig. 11. Temperature distribution at crank angle of 510°.

walls is heated by the walls which are at higher temperature. The gas will be at the lowest temperature at the core region of the working chamber because it is thermally furthest from the hotter walls. The temperature in this region increases subsequently mainly as a consequence of compression process. As the gas pressure increases further, energy is transferred to the gas resulting in further increase in the gas temperature. With additional effect from heat transfer, the temperature of gas near the walls rises rapidly to exceed the scroll wall surface temperature. The gas has the higher temperature at the narrow regions of two apexes than that at other regions. This is because the most significant heat transfer occurs at these narrow regions due to a highly turbulent gas motion and steep velocity gradient between the gas and the walls that result in a high heat transfer coefficient. It should be noticed that the above calculation was based on the assumption of a uniform temperature for fixed and orbiting scroll wall because of complexity of this problem. This assumption implied that the heat conduction across wall was neglected and the problem has been simplified to focus on the fluid flow and its effect on the convective heat transfer. More comprehensive analyses that consider both the conduction and the convective heat transfer are expected in future studies.

3.4. Heat transfer

3.4.1. Surface averaged heat transfer coefficient

The convective heat transfer between the gas and the scroll wrap walls is driven by fluid motions and the heat transfer coefficient depends strongly on the strength of the fluid motions such as velocity and the intensity of turbulence. Inspection of Eq. (8) and computation results show that the convective heat transfer coefficient is mainly governed by the product of $\rho k^{1/2}$ with a modulation of the dimensionless boundary layer thickness y^+, where k is the local turbulent kinetic energy of the gas, ρ is the average boundary layer density. This coincides with Colburn's analogy which assumes a similar heat transfer mechanism, where $U_{\text{eff}} = (U^2 + 2k)^{1/2}$ is the mean effective velocity outside a boundary layer at a particular surface location.

The total spatial averaged heat transfer coefficients versus crank angle at various operating conditions are presented in Figs. 12–15. During the early period of the compression process, the heat transfer coefficient decreases gently. This is because the gas motion intensity and the density have very small variation when the gas began to be compressed. The heat transfer rate rises gradually as the compression process continues beyond the crank angle of about 200°. Although the gas velocity continues to decrease, the effect of turbulent kinetic energy strengthens due to the highly curved geometry of the scroll wall and an increase of the gas density. During the later period of the compression process, the gas density increases drastically and results a sharp rise of heat transfer coefficient. The spatial differences in heat transfer coefficient exist between the walls of the fixed and the orbiting scroll for all operating conditions. For the case of a low suction pressure of 0.1 MPa, there is a higher heat transfer rate at the orbiting scroll wall than that at the fixed scroll.

An increase in the fluid velocity increases the local heat transfer coefficient. The overall effect of increasing the

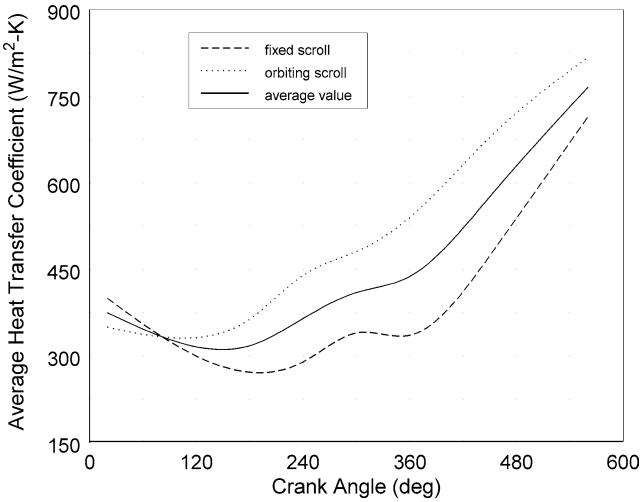

Fig. 12. Average heat transfer coefficient variation versus crank angle $n = 1000$ rev·min, $Ps = 0.1$ MPa.

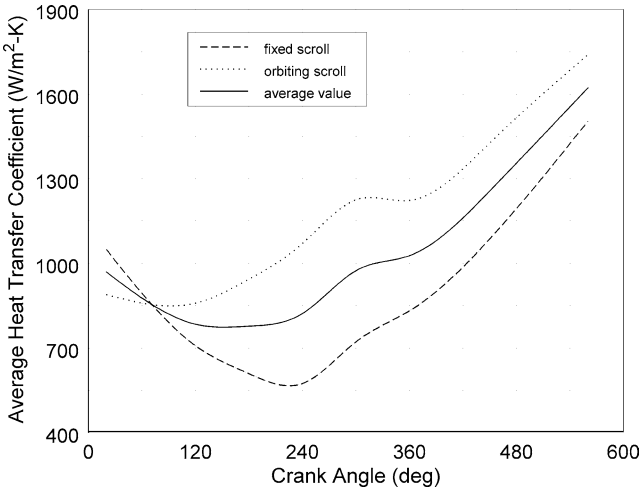

Fig. 13. Average heat transfer coefficient variation versus crank angle $n = 3000$ rev·min, $Ps = 0.1$ MPa.

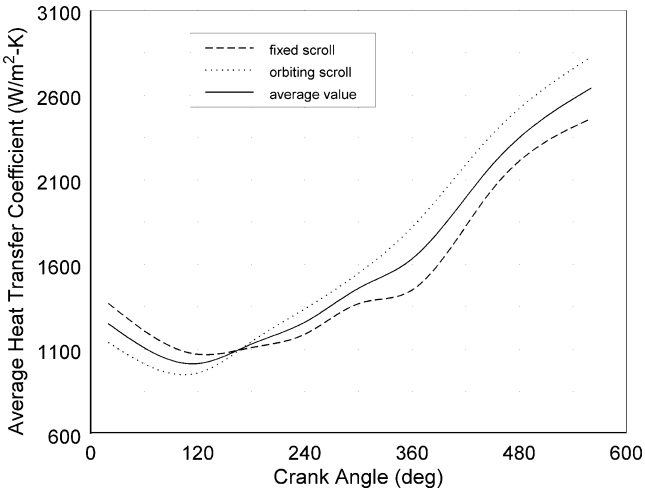

Fig. 14. Average heat transfer coefficient variation versus crank angle $n = 1000$ rev·min, $Ps = 0.35$ MPa.

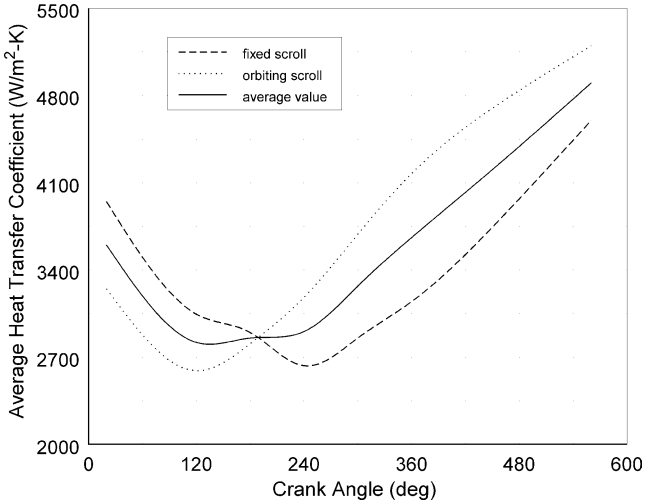

Fig. 15. Average heat transfer coefficient variation versus crank angle $n = 3000$ rev·min, $Ps = 0.35$ MPa.

rotating speed results in an increase in the heat transfer rate between the gas and the scroll surface in the working chamber. For an example, the peak value increases from 800 $W \cdot m^{-2} \cdot K^{-1}$ to 1600 $W \cdot m^{-2} \cdot K^{-1}$ when the compressor speed increases from 1000 to 3000 $rev \cdot min^{-1}$. This reveals a non-linear relationship between the heat transfer coefficient and the compressor rotating speed. The heat transfer is enhanced with speed because of an increase in the gas motion intensity. The individual contribution from these effects to heat transfer depends on various compressor parameters. Increasing the scroll compressor suction pressure increases the gas density and hence increases substantially the surface heat transfer coefficient.

3.4.2. Surface averaged heat flux

Since the convective heat transfer occurs through the boundary layer near the scroll walls, the temperature difference between the wall and the gas is the important parameter which determines the magnitude of the surface heat flux. Before the gas temperature near the wall surfaces exceeds the wall temperature, the thermal energy is transferred from the wall to the boundary layer and it is stored there. Therefore heat flows from the wall to the boundary layer and subsequently from the boundary layer to the core gas as shown in Figs. 16 and 17. At the moment when the core temperature exceeds the wall temperature, the gas temperature in the boundary layer can be higher than the wall. Thus, there is heat flow from the boundary layer to the wall and to the core gas, simultaneously. The results also show that during the first half of the compression process, the heat flux increases non-linearly with rotating speed. At a low rotating speed range, the heat flux increases significantly with speed. This indicates that the gas motion intensity therefore the heat transfer coefficient is a dominant factor. While at high rotating speeds, the temperature difference determines to a large extent the heat flux. Increasing the scroll compressor suction

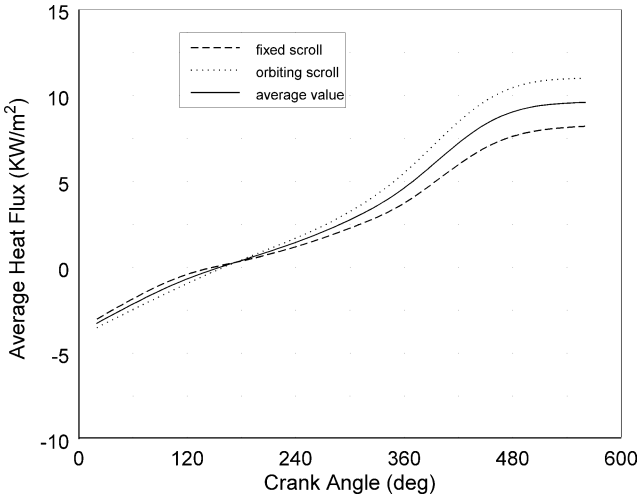

Fig. 16. Surface averaged heat flux variation versus crank angle $n = 1000$ rev·min, $Ps = 0.1$ MPa.

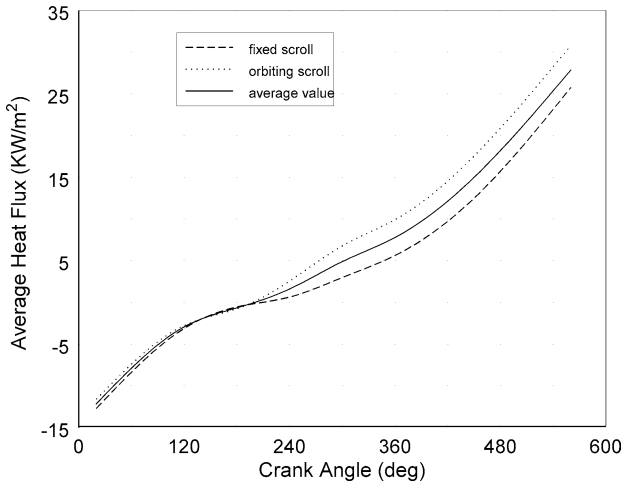

Fig. 17. Surface averaged heat flux variation versus crank angle $n = 3000$ rev·min, $Ps = 0.1$ MPa.

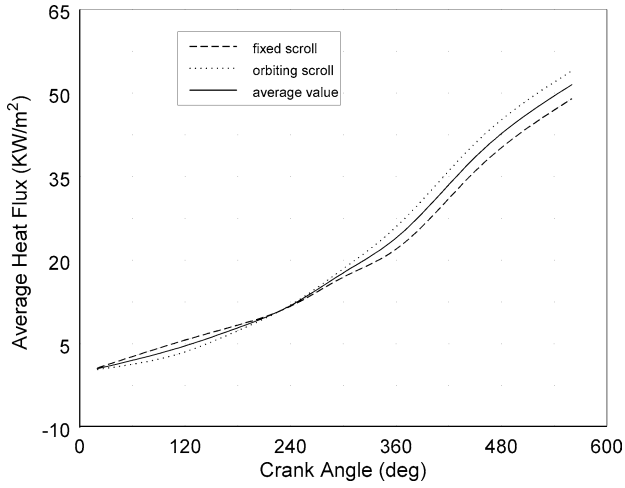

Fig. 18. Surface averaged heat flux variation versus crank angle $n = 1000$ rev·min, $Ps = 0.35$ MPa.

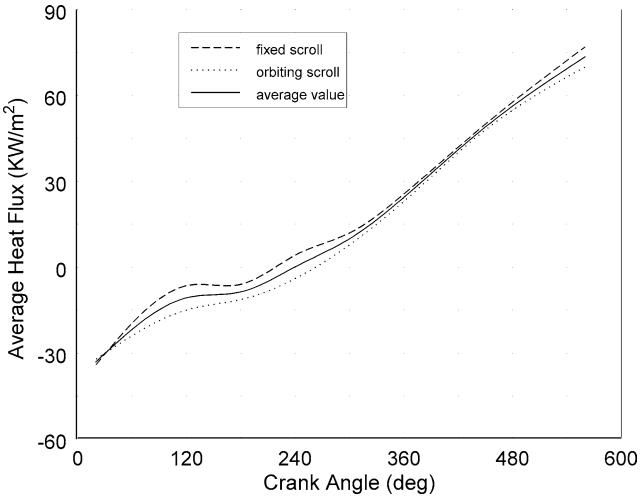

Fig. 19. Surface averaged heat flux variation versus crank angle $n = 3000$ rev·min, $Ps = 0.35$ MPa.

pressure also increases substantially the surface heat transfer coefficient and thus the heat flux as shown in Figs. 18 and 19.

3.4.3. Comparison with empirical correlations

As mentioned earlier, most thermodynamic models employed empirical correlations to estimate the effect of the instantaneous heat transfer on the thermodynamic performance of compressors. To evaluate the suitability of those models for scroll compressor, a comparison is given between numerical results and heat transfer calculations using several empirical correlations. The widely used models among the famous ones include those from Annald [7], Woschni [8] and Adair [9]. Some have been employed directly to estimate the heat transfer in reciprocating compressor and other rotary machinery. All these correlations follow the analogy between heat and momentum transfer in fully developed turbulent boundary layer flow in duct, where the functional relationship is approximately similar with those for turbulent pipe and flat plate boundary layer flows.

The numerical results are presented in terms of the total surface averaged heat transfer coefficient and heat flux in order to facilitate the comparison with predictions using a lumped parameter approach. As shown in Figs. 20 and 21, the instantaneous heat transfer from the 2-D simulation was significantly higher than most of those predicted by empirical correlations except that using the Annald's model. In the case when the operating speed is at 3000 rev·min^{-1}, the average heat transfer coefficient predicted using 2-D model was about two times that predicted by Woschni's and Adair's correlations. This large discrepancy is due to the effect of the geometry deformation of the highly curved scroll chamber which strongly affects the turbulence flow and convective heat transfer characteristics. The empirical correlations used in the lumped parameter model assume that convective heat transfer is only a function of Reynolds and Prandtl number. Therefore prediction using those empirical correlations

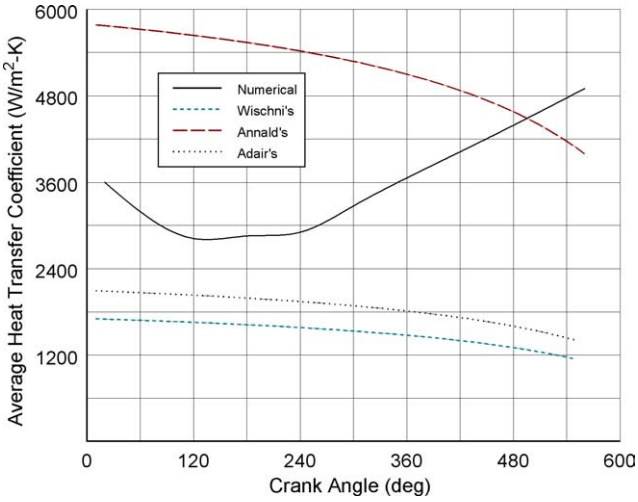

Fig. 20. Comparison of surface averaged heat transfer coefficient with the empirical correlations ($n = 3000$ rev·min, $Ps = 0.35$ MPa).

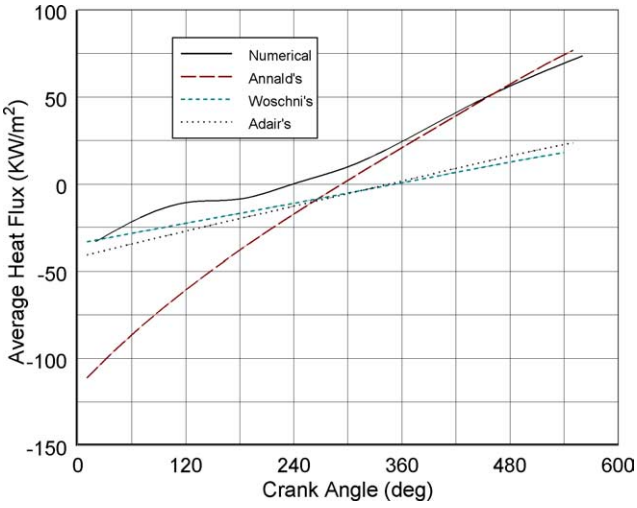

Fig. 21. Comparison of surface averaged heat flux with the empirical correlations ($n = 3000$ rev·min, $Ps = 0.35$ MPa).

shows that in the late period of the compression process, the heat transfer coefficient decreases with reductions in the gas velocity. However, in the numerical prediction, the turbulence effects are particularly strong during the late period of the compression process, where the re-circulating flow is most apparent. This resulted in a significant increase of the heat transfer. For an averaged heat flux calculation, large discrepancies also exist between the predictions by empirical correlations and the 2-D model. Before the crank angle of 400°, it appears that the heat flux predicted by Woschni's and Adair's model is reasonably close with the numerical results, but the discrepancy becomes larger as the crank angle increases. After the crank angle of 400°, Annald's model appears to give better agreement with the numerical predictions. The comparison suggests that no single empirical correlation is completely suitable for the heat transfer evaluation for the whole compression process.

In summary, the numerical simulation results suggest that there exists significant convective heat transfer effect on compression process of a scroll compressor. It is worth to mention again that the present model is based on the assumptions that the effects of leakage and lubricating oil on the compression process and heat transfer were neglected. However, there can be significant heat transfer to the lubricating oil and the leakage between compression chambers and surrounding is also a loss mechanism for scroll compressors. The current work concentrated on obtaining a basic understanding on the fluid flow and convective heat transfer in a scroll chamber by separating the thermal effect of the cycle from the effect of leakage and oil. More comprehensive study on the effects of both leakage and lubricating oil on the heat transfer and compression process would be a worthwhile pursuit in future studies.

4. Conclusions

A two-dimensional numerical model has been formulated to simulate the fluid flow and heat transfer inside a scroll compressor working chamber. The results show that the flow field is determined by the scroll chamber geometry and the operational speed of the compressor. Due to the strong squish motion of the orbiting scroll, unidirectional velocity field of the gas is maintained until the re-circulating flow occurs during the later period of the compression process, where high velocity gradient and turbulence intensity were predicted.

The results reveal that the gas pressure is reasonably uniform and it is consistent with the general assumption in compressor working process simulation using the lumped parameter approach. But all other gas properties show highly non-uniform spatial distributions. The gas temperature is spatially non-uniform particularly at the region near the two apexes and the scroll chamber walls. Maximum temperature difference of 8K was predicted within the working chamber. The results show that the gas temperature was strongly affected by not only the compression effect but also by the convective heat transfer between the gas and the scroll walls.

This 2-D numerical model predicted a significant higher convective heat transfer between the gas and scroll wrap walls than that predicted using the empirical correlations. During the late period of the compression process, the heat transfer coefficient increases gradually with crank angle rather than decreases as predicted using the empirical correlations. Results also show that the turbulence intensity instead of the gas velocity is a main factor governing the heat transfer. The magnitude of heat transfer increases with the operating pressure and the rotating speed. It is therefore concluded that heat transfer should be considered in order to improve the accuracy of the simulation in the thermodynamic process in the scroll compressor and, the existing empirical correlations are inadequate and therefore unsuitable for the convective heat transfer prediction within the

scroll compressor working chamber. More comprehensive studies on the effects of both leakage and lubricating oil on the convective heat transfer and compression process are expected in the future work.

References

[1] L.C. Jean, A computer model for scroll compressor, in: Proceedings of 1988 International Compressor Engineering Conference, Purdue University, 1998, pp. 47–55.
[2] Y. Chen, P. Halm N, E.A. Groll, J.E. Braun, Mathematical modeling of scroll compressors—Part I: Compression process modeling, Internat. J. Refrigeration 25 (2002) 731–750.
[3] Y. Chen, P. Halm N, E.A. Groll, J.E. Braun, Mathematical modeling of scroll compressors—Part II: Overall scroll compressor modeling, Internat. J. Refrigeration 25 (2002) 751–764.
[4] E.L. Winandy, J. Lebrun, Scroll compressors using gas and liquid injection: experimental analysis and modelling, Internat. J. Refrigeration 25 (2002) 1143–1156.
[5] G.H. Lee, Performance simulation of scroll compressors, J. Institution Mech. Engrg. A 216 (2002) 169–179.
[6] N.J. Stosic, I.K. Smith, S. Zagorac, CFD studies of flow in screw and scroll compressors, in: Proceeding of 1996 International Compressor Engineering Conference, vol. 1, Purdue University, 1996, pp. 181–186.
[7] J.D. Annald, Heat transfer in the cylinder of reciprocating internal combustion engine, in: Proc. Internat. Mech. Engrg., vol. 177, 1963, pp. 973–990, No. 36.
[8] G. Woschni, A universally applicable equation for the instantaneous heat transfer coefficient in the internal combustion engine, SAE Trans. 670931 (1967).
[9] R.P. Adair, E.B. Qvale, J.T. Pearson, Instantaneous heat transfer to the cylinder wall in reciprocating compressor, in: Proceeding of 1972 Purdue Compressor Technology Conference, Purdue University, 1972, pp. 521–526.
[10] S.V. Patankar, Numerical Heat Transfer and Fluid Flow, McGraw-Hill, New York, 1980.
[11] B.E. Launder, D.B. Spalding, The numerical computation of turbulent flows, Comput. Methods Appl. Mech. Engrg. 3 (1974) 269–289.
[12] R.E. Smith, Two-boundary grid generation for the solution of the three-dimensional Compressible Navier–Stokes equations, NASA Technical Memorandum, 1981, Publication No. 83123.
[13] S.L. Yang, T. I-P. Shih, An algebric grid generation technique for time-varying two-dimensional spatial domains, Internat. J. Numer. Methods Fluid 6 (1986) 291–403.
[14] T.I.-P. Shih, S.L. Yang, H.J. Schock, A Two-dimensional numerical study of the flow inside the combustion chambers of a motored rotary engine, SAE Trans. 860615 (1986).
[15] H. Tennekes, J.L. Lumley, A First Course in Turbulence, MIT Press, Cambridge, MA, 1974.
[16] P. Gilaber, P. Pinchon, Measurements and multidimensional modelling of gas-wall heat transfer in a S.I. engine, SAE Trans. 880516 (1988).
[17] A.D. Gosmen, Computer modelling of flow and heat transfer in engines, progress and prospects, COMODIA 1985 Symposium, JSME, SAEJ, MESJ, Tokyo, 1985.
[18] M. Ikegami, Y. Kidoguchi, K. Nishawaki, A multidimensional model prediction of heat transfer in non-fired engines, SAE Trans. 860467 (1986).
[19] ASHRAE Inc., Heat, ventilating and air-conditioning systems and equipment, in: 2000 ASHARE Handbook. Atlanta, USA, Part 34.21, 2000.